Verification of Limit Equilibrium Methods (LEM)

Ching-Chuan Huang

Professor Emeritus
Department of Civil Engineering,
National Cheng Kung University, Tainan, Taiwan
Email: samhcc@mail.ncku.edu.tw
2025/08/24

INTRODUCTION

SLOPE-ffdm 2.0 is a Windows-based computer program designed to evaluate slope stability and predict potential displacements in both natural and man-made slopes. It offers two key functions:

1. **Slope Stability Analysis** – Utilizes various limit equilibrium methods, including Fellenius, Bishop, Morgenstern-Price, Spencer, and Janbu, to assess stability.
2. **Slope Displacement Calculation** – Employs the Force-Equilibrium-Based Finite Displacement Method (FFDM), as detailed in Series 1 and Series 4– 7, to estimate slope movements.

This report series focuses on verifying the accuracy of the limit equilibrium methods using well-documented case studies. Comparative analysis indicates that the safety factor (Fs) for a given failure surface, as computed by SLOPE-ffdm 2.0, deviates from published values by no more than 3%, an acceptable margin. Additionally, F_s values obtained through trial-and-error searches for critical surfaces tend to be slightly lower than those reported in the literature. These findings affirm the accuracy and reliability of SLOPE-ffdm 2.0's formulation and computational algorithms

3.1 VERIFICATION CASE STUDY NO. 1

Input file path: *\SLOPE-ffdm 2.0\Docs\example_verification\Ch3.1

verification_type-1_Duncan&Wright_Fig.7.6_input.txt
verification_type-2_Duncan&Wright_Fig.7.6_input.txt
verification_type-3_Duncan&Wright_Fig.7.6_input.txt

Output file path: *\SLOPE-ffdm 2.0\Docs\example_verification\Ch3.1

verification_type-1_Duncan&Wright_Fig.7.6_output.txt
verification_type-2_Duncan&Wright_Fig.7.6_output.txt
verification_type-3_Duncan&Wright_Fig.7.6_output.txt

This analysis examines a vertical cut in varved clay, considering assumed tension crack depths ranging from 0 to 4 feet (Figure 7.6 in Duncan and Wright, 2005). Type-1 analysis in SLOPE-ffdm 2.0, using a grid of rotation centers, is illustrated in Figure 3.1.1. A total of 1,349 trial-and-error circular failure surfaces were evaluated.

The input data file includes five scenarios with varying tension crack depths. Figure 3.1.2 presents the critical failure surfaces identified using Fellenius, Bishop, and Spencer's methods. In the case of $\boldsymbol{\phi = 0}$ analysis, all three methods yield identical safety factor (F_s) values.

Table 3.1.1 compares the F_s values obtained in Type-1 analysis with those reported in the literature, demonstrating strong agreement between the computed and published results.

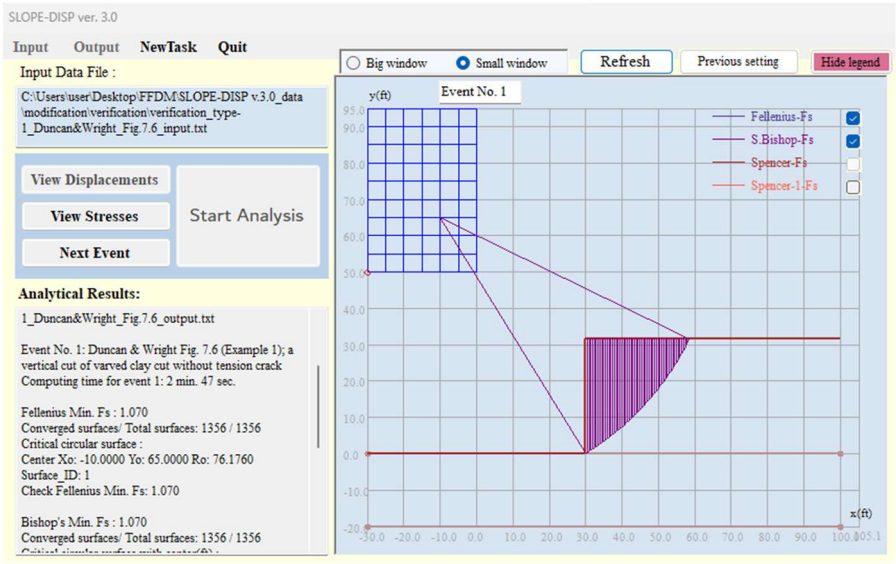

Figure 3.1.1 Graphics for the result of analysis for event 1

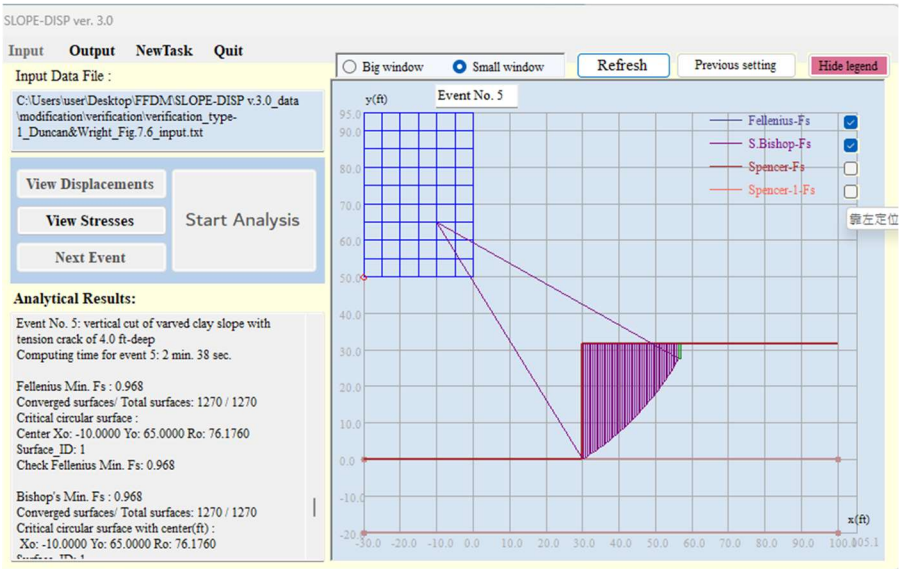

Figure 3.1.2 Graphics for the result of analysis for event 5 with a 4.0 ft-deep tension crack

Table 3.1.1 Safety factors calculated by Type-1 analysis and those reported by Duncan and Wright (2005)

Depth of tension crack (ft)	F_s by Duncan and Wright (2005)	F_s by SLOPE-ffdm 2.0
0	1.06	1.070
1	1.04	1.043
2	1.01	1.017
3	0.99	0.992
4	0.96	0.968

To assess the integrity of SLOPE-ffdm 2.0, additional analyses were conducted using Type-2 (passing-through-a-point circular surface) and Type-3 (single circular surface) methods.

In the Type-2 analysis, the grid of rotation centers remained the same as in Type-1, with the slope toe (30.0, 0.0) serving as the passing-through point. The resulting safety factor (F_s) values are summarized in Table 3.1.2 which shows slightly lower values of F_s than those shown in Table 3.1.1. This highlights the effectiveness of Type-2 analysis—particularly for vertical cuts—by providing more efficient and precise results through toe-constrained failure surface evaluations.

The analysis incorporated two soil strata:

- **Layer 1 (topmost layer):** Undrained shear strength $\mathbf{c_u = 1050\ psf}$, $\mathbf{\phi = 0°}$
- **Layer 2 (bottom layer):** High-strength properties $\mathbf{c_u = 3000\ psf}$, $\mathbf{\phi = 40°}$, assigned to prevent deep failure below the toe.

Table 3.1.2 summarizes the minimum Fs values obtained from Type-1, Type-2, and Type-3 analyses. Notably, in the Type-3 (single-circle) analysis, the input rotation center and radius were derived from the critical values obtained in Type-2. Consequently, Type-2 and Type-3 analyses yielded identical Fs values, thereby confirming the reproducibility of analytical procedures in SLOPE-ffdm 2.0.

Table 3.1.2 F_s calculated by Type-1, Type-2 and Type-3 analyses

Depth of tension crack (ft)	F_s by Type-1	F_s by Type-2	F_s by Type-3
0	1.070	1.064	1.064
1	1.043	1.037	1.037
2	1.017	1.011	1.011
3	0.992	0.986	0.986
4	0.968	0.961	0.961

3.2 VERIFICATION CASE STUDY NO. 2

Input and output path: *\SLOPE-ffdm 2.0\Docs\example_verification\Ch3.2

Input: verification_type-1_Duncan&Wright_Fig.7.7_input.txt
Output: verification_type-1_Duncan&Wright_Fig.7.7_output.txt

This case study examines an underwater slope failure in San Francisco Bay mud, originally reported by Duncan and Buchignani (1973). A portion of the slope collapsed during construction. The reported undrained strength profile: a saturated unit weight of γ_{sat} = 100.4 pcf, with an undrained strength at the mud surface of cu_o = 98.2 psf and an increasing rate of $\Delta c_u/\Delta z$ = 10.145 psf/ft. For the debris dike, γ_{sat} = 87.4 pcf and a uniform undrained strength of c_u = 800 psf.

Spencer's method was used in the original study to estimate the factor of safety (F_s), yielding F_s = 1.17, although the critical failure surface was not specified. Table 3.2.1 presents Fs values derived from a Type-1 analysis using SLOPE-ffdm 2.0. All methods applied—Fellenius, Bishop, and Spencer—produced consistent results with Fs = 1.192, corresponding to the same critical failure surface shown in Fig. 3.2.1.

The calculated Fs of 1.192 differs from the previously reported value by only 1.9%, lending confidence to the computational reliability of the SLOPE-ffdm 2.0 algorithm. This minor discrepancy likely stems from variations introduced during digitization of the original slope profile from printed documents.

Table 3.2.1 also highlights an important feature of the computer program: the use of submerged soil unit weight (via the "water table" command with ID = 3) and total unit weight reflecting hydrostatic water pressures (via the "water table" command with ID = 4) resulted in identical failure surfaces (Figs. 3.2.1 and 3.2.2) and F_s values (Table 1.2.1) regardless of the slice methods used. This consistency suggests that porewater pressure effects are accurately accounted for in computations.

Table 3.2.1 F_s based on different considerations of porewater pressures

F_s reported by Duncan and Buchignani (1973)	F_s using Submerged unit weight (Event 1)	F_s using Hydrostatic pressure (Event 2)
1.17	1.192	1.192

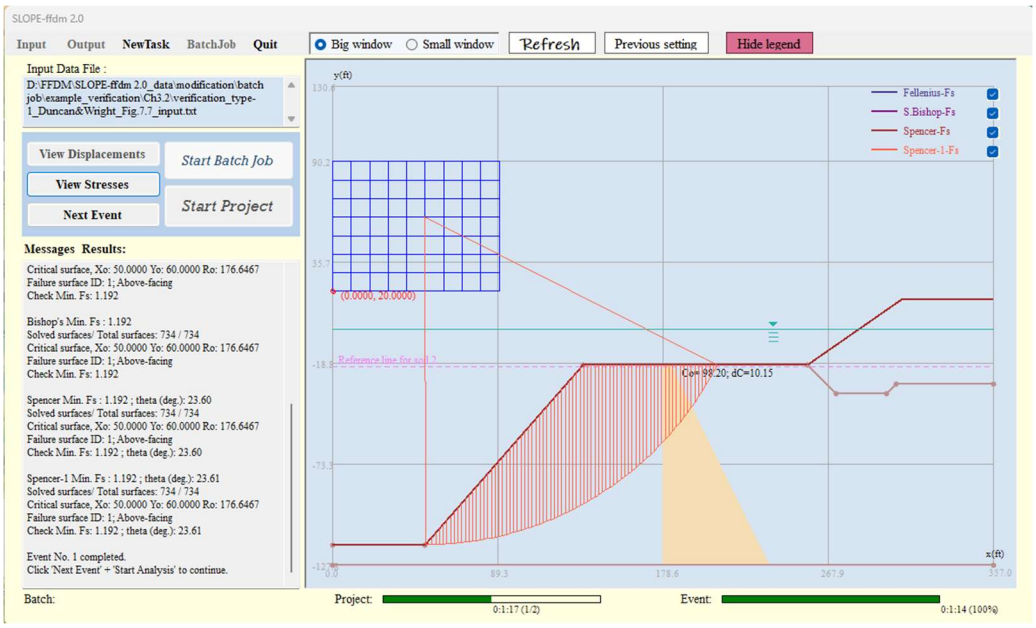

Figure 3.2.1 Critical surface found in 734 trial-and-error arcs using submerged unit weight of soils

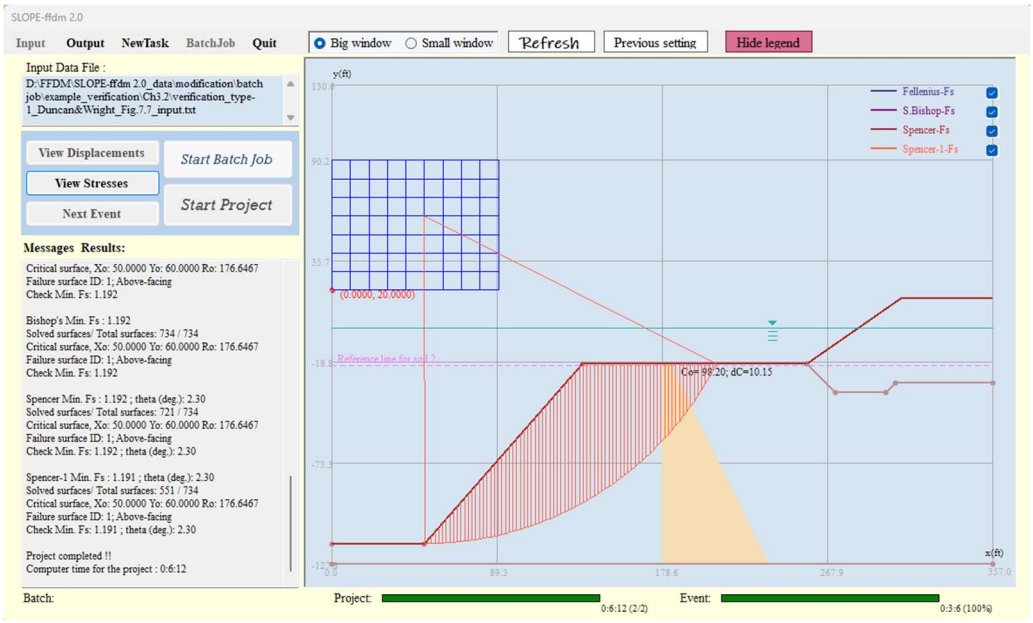

Figure 3.2.2 Critical surface found in 734 trial-and-error arcs using saturated unit weight of soils and hydrostatic porewater pressures

3.3 VERIFICATION CASE STUDY NO. 3

Input and output path: *\SLOPE-ffdm 2.0\Docs\example_verification\Ch3.3

Input: verification_type-1_Duncan&Wright_Fig.7.9_input.txt Input: verification_type-2_Duncan&Wright_Fig.7.9_input.txt
Output: verification_type-1_Duncan&Wright_Fig.7.9_output.txt Output: verification_type-2_Duncan&Wright_Fig.7.9_output.txt

This case study, reported by Duncan and Wright (2005), examines an excavated slope consisting of London clay. The slope is composed of four soil layers: Layer No. 1 (top) is an embankment fill, replaced by an equivalent surcharge due to full-depth cracking; Layer No. 2 has a uniform undrained strength of c_u = 300 psf; Layer No. 3 features a cohesion profile with c_{u_o} = 860 psf at the top and an increasing rate of $\Delta c_u/\Delta z$ = 65 psf/ft; Layer No. 4 begins with c_{u_o} = 2420 psf and increases at a rate of $\Delta c_u/\Delta z$ = 35 psf/ft. Figure 3.3.1 presents the critical failure surface identified through 2,959 trial-and-error searches. All methods implemented in the program (Fellenius, Bishop, Spencer, and Spencer-1) produced identical critical surfaces and a minimum Fs value of 1.714. This value is slightly lower than the F_s = 1.76–1.80 range (Table 3.3.1) reported by Duncan and Wright (2005), reflecting a difference of approximately 2%–5%, which is within an acceptable range.

As summarized in Table 3.3.1, Type-2 analysis (passing-through-a-specific-point analysis) was also conducted by setting the slope toe (x = 20.0, y = –31.0) as the default passing-through point. The minimum F_s value obtained from Type-2 analysis was 1.726, consistent across all methods used, and slightly smaller than that from Type-1 analysis (F_s = 1.731). This result is comparable to Case Study No. 1, which indicated that Type-3 analysis can be more effective for steep slopes that typically exhibit failure surfaces passing through the slope toe.

Table 3.3.1 Comparisons of minimum values of F_s obtained in various studies.

	Duncan and Wright (2005)	Type-1 analysis; SLOPE-ffdm 2.0	Type-2 analysis; SLOPE-ffdm 2.0
F_s	1.76- 1.80	1.731	1.726

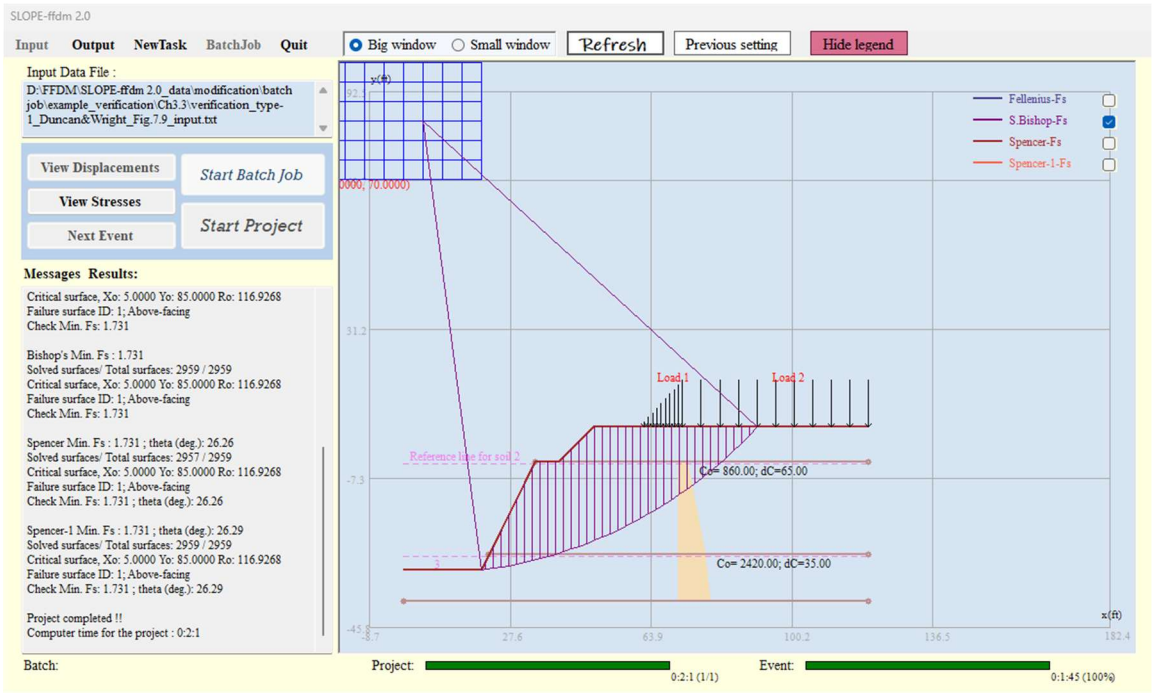

Figure 3.3.1 Critical surface for the slope consisting of London clay (Figure 7.9 of Duncan and Wright, 2005)

3.4 VERIFICATION CASE STUDY NO. 4

Input and output path: *\SLOPE-ffdm 2.0\Docs\example_verification\Ch3.4

Input: verification_type-1_3_Duncan&Wright_Fig.7.12_input.txt
Output: verification_type-1_3_Duncan&Wright_Fig.7.12_output.txt

This hypothetical embankment consists of granular material (c= 0) resting on a saturated clay foundation (ϕ= 0), as illustrated in Fig. 7.12 of Duncan and Wright (2005). The geometry of the critical slip circle is provided, enabling a straightforward comparative study using SLOPE-ffdm 2.0. First, a Type-3 analysis is conducted on the critical circular surface reported by Duncan and Wright (2005), shown in Fig. 3.4.1. The results, summarized in Table 3.4.1, indicate that the computed factor of safety (F_s) is nearly identical to the originally reported value.

To validate the failure mechanism and the safety factor of the slope, a Type-1 analysis was also performed using a trial-and-error search across circular surfaces. These results suggest that the critical surface identified (Fig. 3.4.1) closely resembles but is not identical to- that reported by Duncan and Wright (2005). The minimum F_s values obtained via Type-1 analysis are approximately 0.8–1.5% lower than the original reference value (see Table 3.4.1)

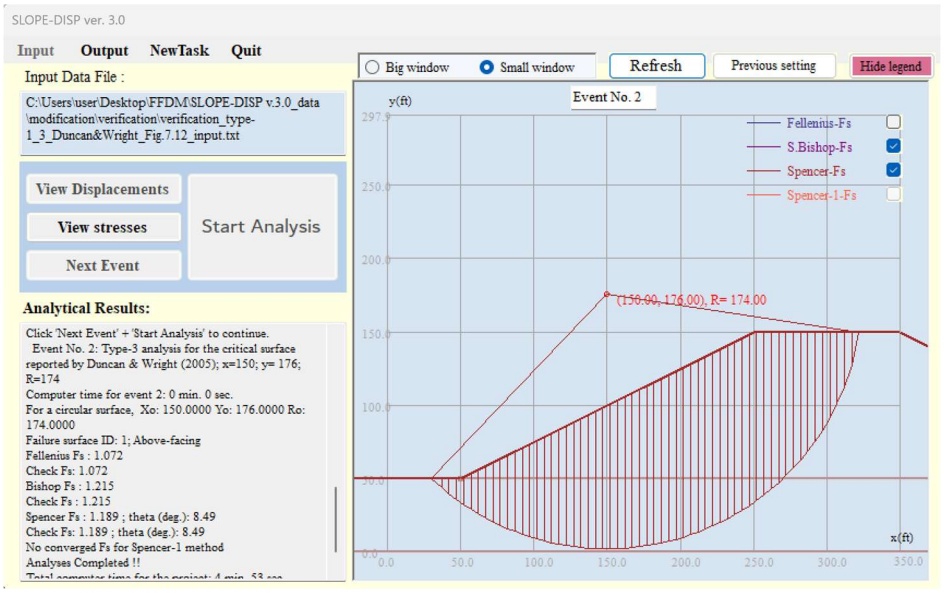

Figure 3.4.1 Type-3 analysis (Event 2 of the input data file) for the critical failure circle reported in Figure 7.12 of Duncan and Wright (2005).

Table 3.4.1 Comparisons of safety factors obtained in various studies.

	Duncan and Wright (2005)	Type-1 analysis	Type-3 analysis
Bishop's F_s	1.22	1.202	1.215
Spencer's F_s	1.19	1.180	1.189

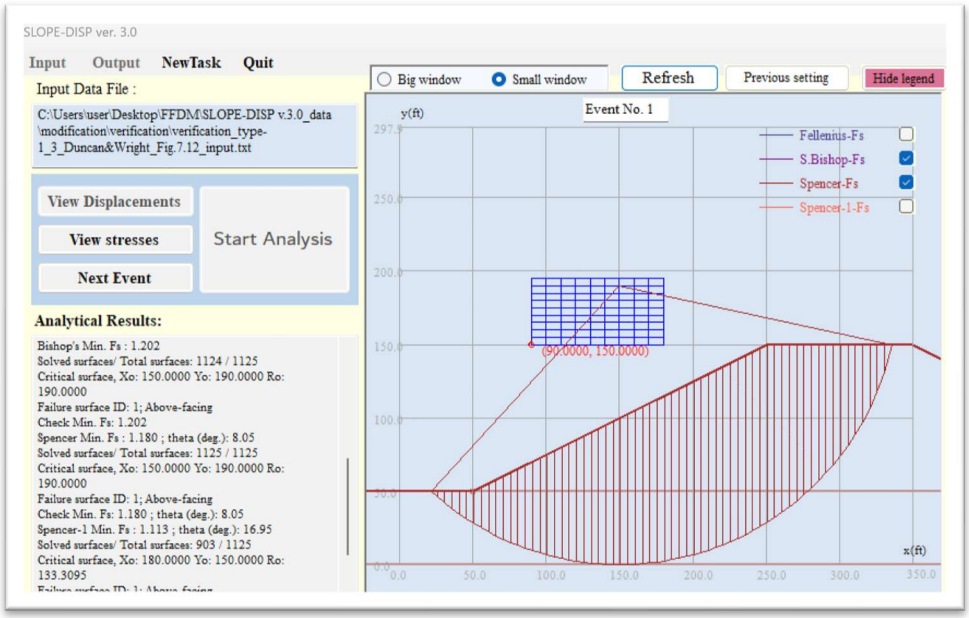

Figure 3.4.2 Critical surface found in Type-1 analysis (Event 1 of the input data file)

3.5 VERIFICATION CASE STUDY NO. 5

Input and output path: *\SLOPE-ffdm 2.0\Docs\example_verification\Ch3.5

Input: verification_type-1_Duncan&Wright_Fig.7.14_input.txt
Output: verification_type-1_Duncan&Wright_Fig.7.14_output.txt

This study examines the downstream slope stability of Oroville Dam (Fig. 7.14 of Duncan and Wright, 2005). The slope comprises rock fill material characterized by a curved (nonlinear) Mohr-Coulomb failure envelope. For cohesionless materials, the curved failure envelope is often represented by the following equation:

$$\varphi = \varphi_0 - \Delta\varphi \cdot log\frac{\sigma_3'}{p_a} \qquad (3-5-1)$$

φ: internal friction angle
φ_0: internal friction angle at confining pressures lower than pa
p_a: atmospheric pressure
$\Delta\varphi$: rate of internal friction angle reduction per logarithmic cycle of pressure increase
σ'_3: effective minor principal confining pressure

In limit-equilibrium-based stability analyses, values of σ'_n along the slip surface are known, while σ'_3 are usually unknown. Based on a stress analysis using Mohr circles for the downstream shell material of Oroville Dam, Duncan and Wright (2005) proposed the following relationship:

$$\sigma_3' = \frac{\sigma_n'}{b_n} \qquad (3-5-2)$$

Where b_n is a factor between 1.5 and 1.8. Substituting Eqs. (3-5-2) into (3-5-2) yields:

$$\varphi = [\varphi_0 + logb_n \cdot \Delta\varphi] - \Delta\varphi \cdot log\frac{\sigma_n'}{p_a} \qquad (3-5-3)$$

Using Eq. 3-5-3, varying the bracketed term, allows consideration of different b_n (= 1.0, 1.5 and 1.8) and $\Delta\varphi$ values can be considered within SLOPE-ffdm 2.0 analyses. Applying the reported values of φ_0= 51°, $\Delta\varphi$= 6° and the b_n values, Type-1 analyses for Events 1 through 4 are summarized in Table 3.5.1.

Results indicate that increasing the value of b_n from 1.5 to 1.8 has a negligible effect on the minimum safety factor (F_s). Event 1 which assumes b_n= 1.0 (i.e., $\sigma'_3 = \sigma'_n$.) shows less than 1% error in F_s compared to Event 3. However, ignoring the curved

Mohr-Coulomb envelope entirely- as seen when comparing Event 1 and 4- leads a significant overestimation of F_s for 16-17% and produces a shallower critical surface (refer to Figs. 3.5.1 and 3.5.2).

Table 3.5.1 Comparisons of safety factors obtained in various studies.

	Duncan and Wright (2005)	Event 1 ($\Delta\varphi$= 6°, b_n= 1.0)	Event 2 ($\Delta\varphi$= 6°, b_n= 1.5)	Event 3 ($\Delta\varphi$= 6°, b_n= 1.8)	Event 4 ($\Delta\varphi$= 0°)
Bishop F_s	-	2.199	2.207	2.210	2.577
Spencer F_s	2.28	2.198	2.206	2.210	2.577

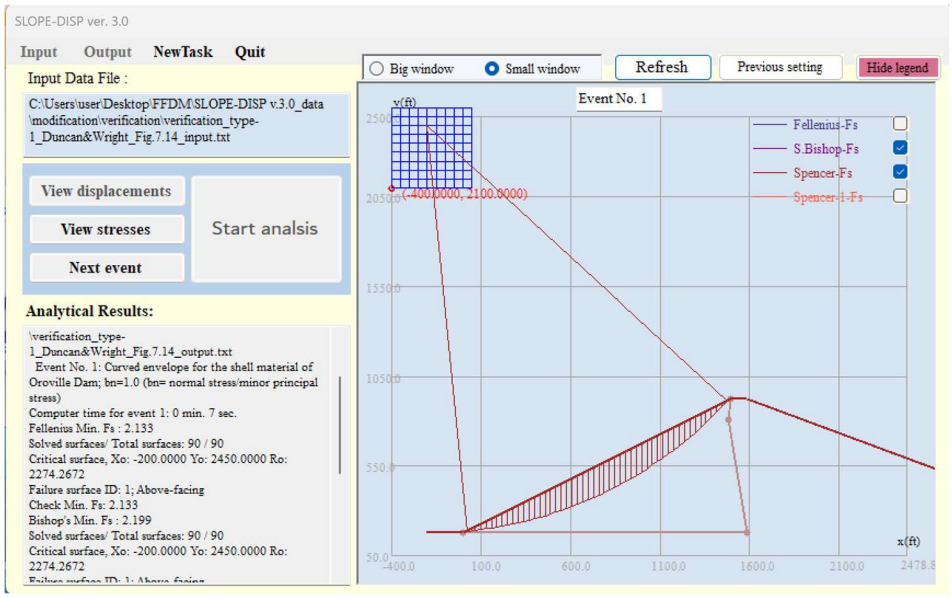

Figure 3.5.1 Critical circular surface found in Event 1 of trial-and-error analysis considering curved Mohr-Coulomb failure envelope with $\Delta\varphi$= 6° and b_n= 1.5.

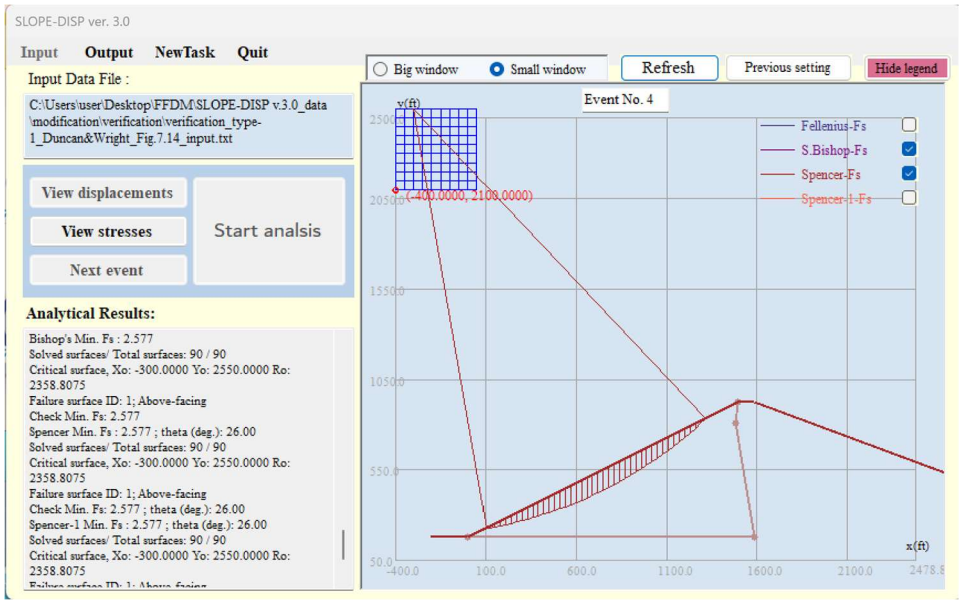

Figure 3.5.2 Critical circular surface found in Event 4 of trial-and-error analysis considering a straight line Mohr-Coulomb failure envelope ($\Delta\varphi$= 0°).

3.6 VERIFICATION CASE STUDY NO. 6

Input and output path: *\SLOPE-ffdm 2.0\Docs\example_verification\Ch3.6

Input: verification_type-1_7_Duncan&Wright_Fig.7.16_input.txt
Output: verification_type-1_7_Duncan&Wright_Fig.7.16_output.txt

This case study investigates the stability of a 12 m-high embankment—the James Bay Dike—constructed over multi-layered soft clay strata. Duncan and Wright (2005) report the following results based on Spencer's procedure:

1. **Circular failure analysis** yielded a minimum factor of safety (F_s) of 1.45.
2. **Noncircular failure analysis** resulted in a minimum F_s of 1.17.

To replicate these conditions using SLOPE-ffdm 2.0, a **Type-1 analysis (Event 1)** was performed corresponding to the circular failure mode. The resulting minimum F_s was 1.462, approximately 0.8% higher than the reported value.

To simulate the noncircular failure condition, a **Type-7 analysis (Event 2)**—accounting for composite failure mechanisms—was conducted. This yielded a minimum F_s of 1.157, 1.1% lower than the value reported by Duncan and Wright.

Table 3.6.1 summarizes the Fs values obtained through different analytical procedures. The critical failure surfaces identified in Type-1 and Type-7 analyses are illustrated in Fig. 3.6.1 and Fig. 3.6.2, respectively. Both the computed safety factors and the failure geometries closely align with those documented in previous literature.

Table 3.6.1 Comparisons of *Fs* for James Bay dike obtained in various studies.

	Duncan and Wright (2005), F_s (Spencer's method)	SLOPE-ffdm 2.0 F_s (Spencer's method)
Critical circular surface	1.45	1.462 (Event 1: type-1 analysis)
Critical composite surface	1.17	1.157 (Event 2: type-7 analysis)

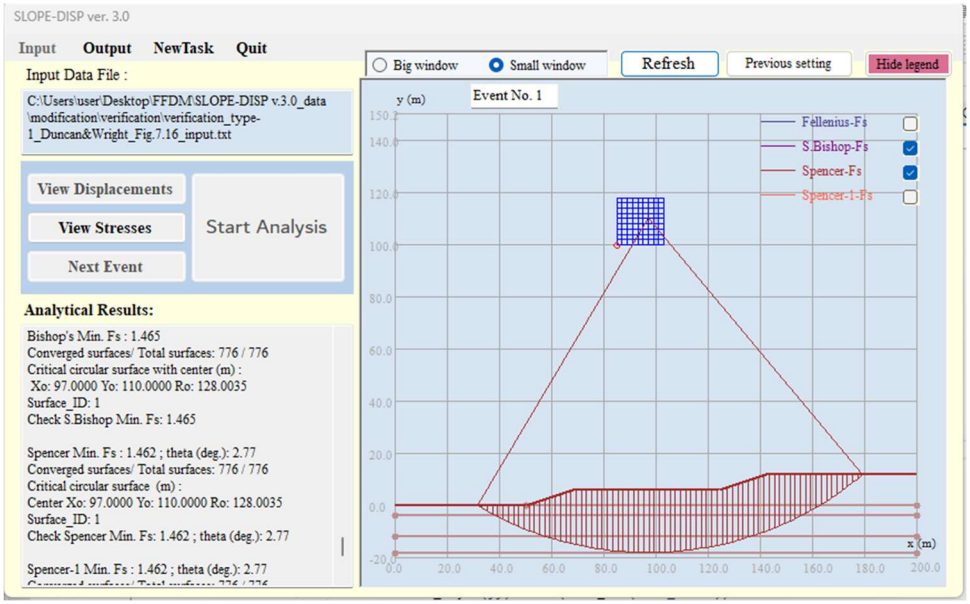

Figure 3.6.1 Critical surface obtained in Event 1 (type-1 analysis) of SLOPE-ffdm 2.0.

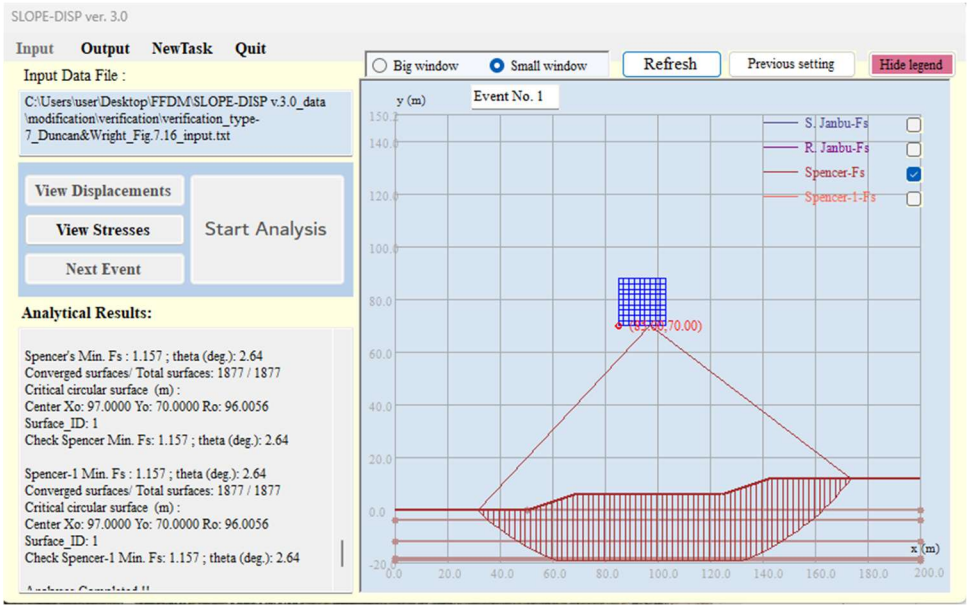

Figure 3.6.2 Critical surface obtained in Event 2 (type-7 analysis) of SLOPE-ffdm 2.0.

3.7 VERIFICATION CASE STUDY NO. 7

Input and output path: *\SLOPE-ffdm 2.0\Docs\example_verification\Ch3.7

Input: verification_type-1_Duncan&Wright_Fig.7.19_input.txt
Output: verification_type-1_Duncan&Wright_Fig.7.19_output.txt

This analysis involves a 48-foot-high homogeneous embankment with material properties defined as c= 100 psf, φ'=30, γ= 100 pcf. The embankment impounds water on one side and experiences steady-state seepage on the downstream side. The phreatic surface and the piezometric line are assumed to coincide.

The phreatic line depicted in Fig. 7.20 of Duncan and Wright (2005) has been digitized and reproduced in Fig. 3.7.1. Two modes of the "water table" command were applied in the SLOPE-ffdm 2.0 stability analysis:

- **Event 1:** Mode-1 (Piezometric line)
- **Event 2:** Mode-5 (Phreatic surface)

Type-1 analysis (trial-and-error search over 644 circular surfaces) using SLOPE-ffdm 2.0 was conducted for Event 1. The resulting factors of safety (F_s) are compared to those reported by Duncan and Wright (2005) in Table 3.7.1. Fs values obtained via Spencer's method are approximately 7– 9% lower than the reference values, likely due in part to discrepancies introduced during the digitization of the phreatic line.

Figures 3.7.1 and 3.7.2 demonstrate that failure surfaces initiating near the downstream slope toe dominate the slope stability. This aligns with established understanding in seepage-related slope failures: the combination of elevated porewater pressure and reduced confining pressure near a saturated toe can trigger failure (Huang et al., 2008). Notably, in the SLOPE-ffdm 2.0 analysis, both Spencer's and Bishop's procedures produced identical critical failure surfaces, as illustrated in Figs. 3.7.1 and 3.7.2.

Table 3.7.1 Comparisons of F_s obtained using piezometric and phreatic lines

	Duncan and Wright (2005) F_s (Spencer's method)	SLOPE-ffdm 2.0 F_s (Spencer's method)	SLOPE-ffdm 2.0 F_s (Bishop's method)
Piezometric line (Event 1)	1.16	1.057	1.050
Phreatic surface (Event 2)	1.24	1.152	1.145

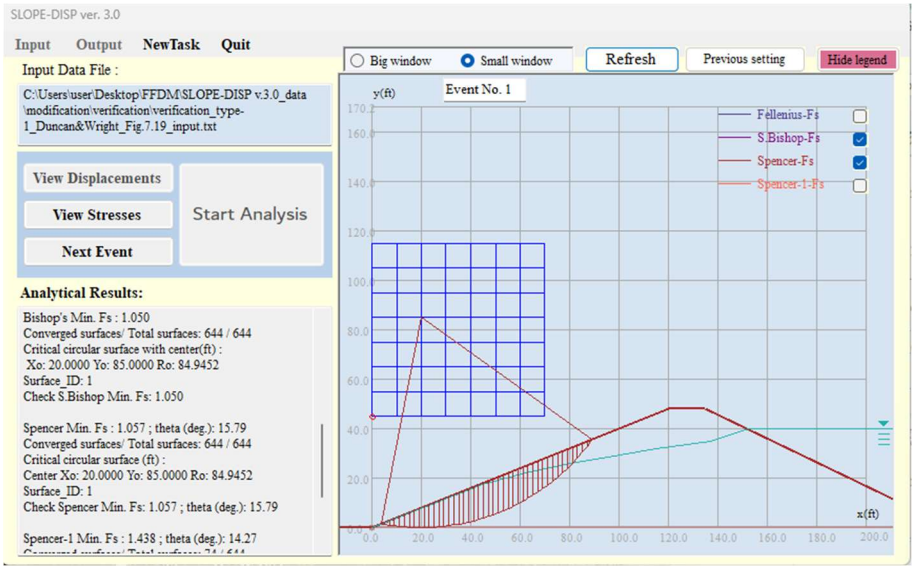

Figure 3.7.1 Critical circular surface for Bishop's and Spencer's methods in Type-1 analysis with the presence of a piezometric line.

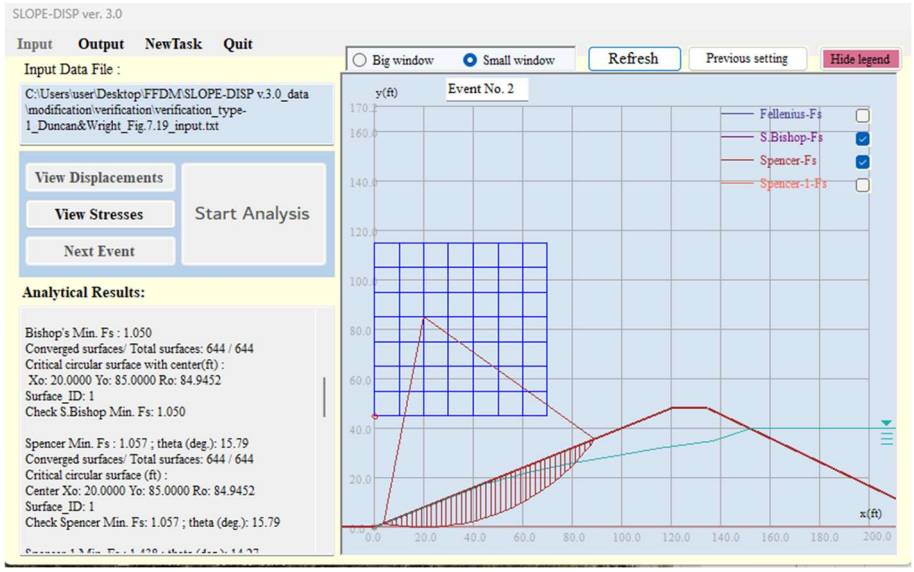

Figure 3.7.2 Critical circular surface for Bishop's and Spencer's methods in Type-1 analysis with the presence of a phreatic surface.

REFERENCE

Huang, C.-C., Lo, C.-L., Jang, J.-S. and Hwu, L.-K. (2008) "Internal soil moisture response to rainfall-induced slope failures and debris discharge" Engineering Geology, 101, 134-145.

3.8 VERIFICATION CASE STUDY NO. 8

Input and output path: *\SLOPE-ffdm 2.0\Docs\example_verification\Ch3.8

Input: verification_type-1_Duncan&Wright_Fig.7.26_input.txt
Output: verification_type-1_Duncan&Wright_Fig.7.26_output.txt

This is a hypothetical reinforced embankment on a clayey foundation. A geosynthetic reinforcement sheet is placed at the bottom of a 6 m-high embankment consisting of cohesionless soil (Soil 1 in this study, Table 3.8.1). The foundation consists of 4 layers of clayey soils with varied undrained shear strength (c_u) expressed in Eq. 3-8-1. The input soil parameters are summarized in Table 3.8.1.

$$c_u = c_{u0} + \Delta c_u \times z \qquad (3-8-1)$$

z: Depth from the top of soil layers

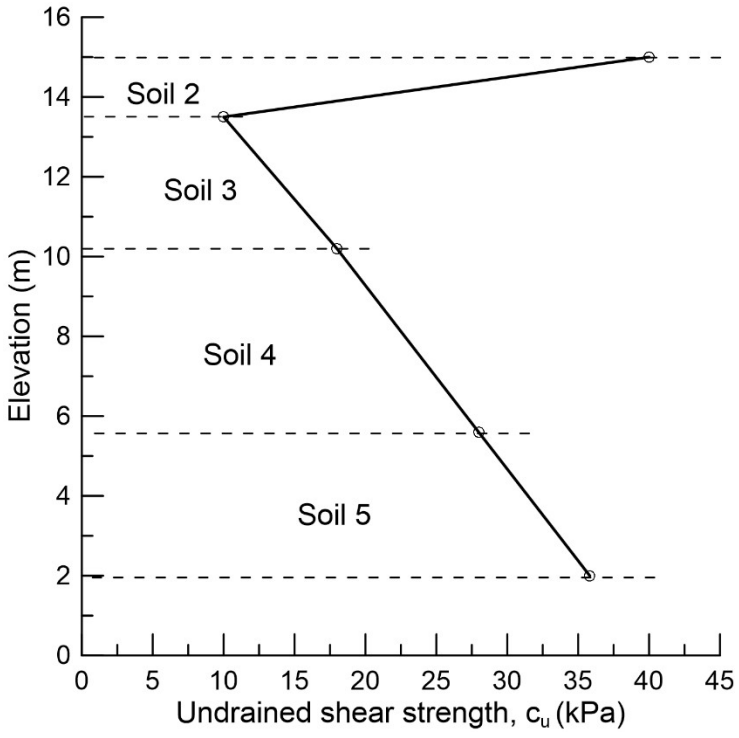

Figure 3.8.1 the undrained shear strength profile for the clayey foundation

Table 3.8.1 Input soil strength parameters for the studied case

Soil layer No.	Elevation (m)	γ (kN/m^3)	φ ($^\circ$)	C_{u0} (kPa)	Δc_u (kPa/m)
1	15.0- 21.0	18.9	44.0	0	0
2	13.5- 15.0	18.4	0	40.0	-20.0
3	10.2- 13.5	16.0	0	10.0	2.42
4	5.6- 10.2	17.0	0	18.0	2.17
5	2.0- 5.6	19.2	0	28.0	2.17
6	1.0- 2.0	19.2	40	50.0	0

Duncan and Wright (2005) reported F_s= 1.13- 1.19 using two computer programs (STABGM and UTEXAS4) with an unknown value of input allowable tensile strength of reinforcement ($T_{allowable}$). Therefore, results of analyses using SLOPE-ffdm 2.0 as summarized in Table 3.8.2 are not intended to make a direct comparison of F_s between the reported and the calculated. Results shown in Table 3.8.2 reveal the fact that minimum values of F_s are influenced by the input value of $T_{allowable}$. The differences of F_s between the Spencer's and Bishop's methods are 1.9- 5.9%.

Critical failure surfaces obtained using Spencer's and Bishop's methods are shown in Figs. 3.8.2, 3.8.3, and 3.8.4 for the cases of $T_{allowable}$= 300, 200 and 100 kN/m. It is interesting to note that the depth of critical surfaces tends to decrease (or becomes shallower) as the input value of $T_{allowable}$ decreases.

Table 3.8.2 Safety factors for a reinforced embankment based on various input tensile strengths of reinforcement.

$T_{allowable}$ (kN/m)	F_s (Spencer's method)	F_s (Bishop's method)
300	1.541	1.478
200	1.298	1.225
100	1.036	1.034

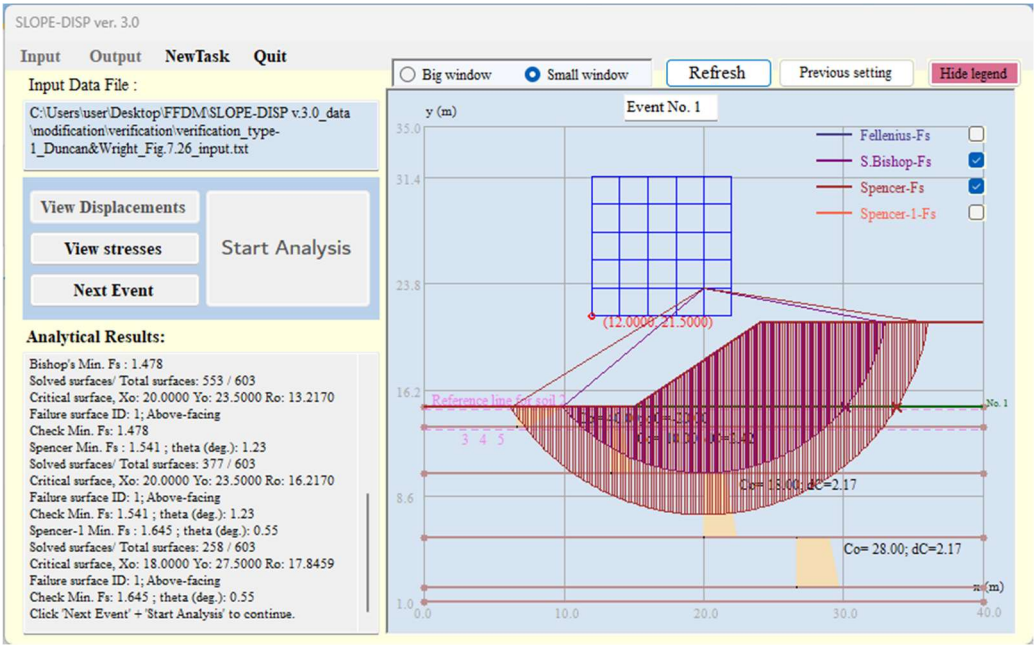

Figure 3.8.2 Critical circular surfaces obtained using Bishop's and Spencer's methods for the case of $T_{allowable}$= 300 kN/m

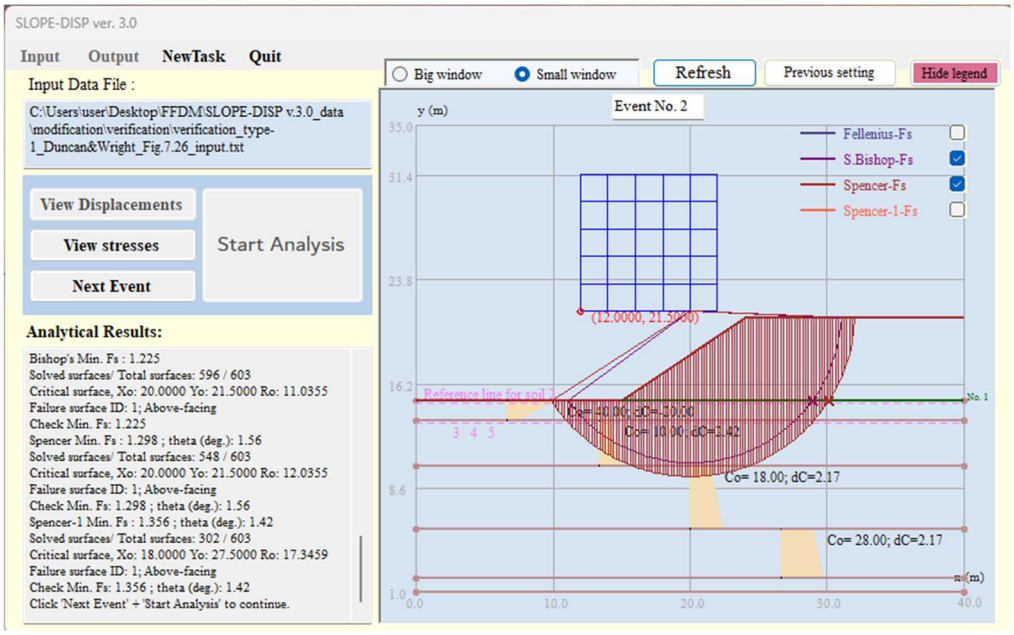

Figure 3.8.3 Critical circular surfaces obtained using Bishop's and Spencer's methods for the case of $T_{allowable}$= 200 kN/m

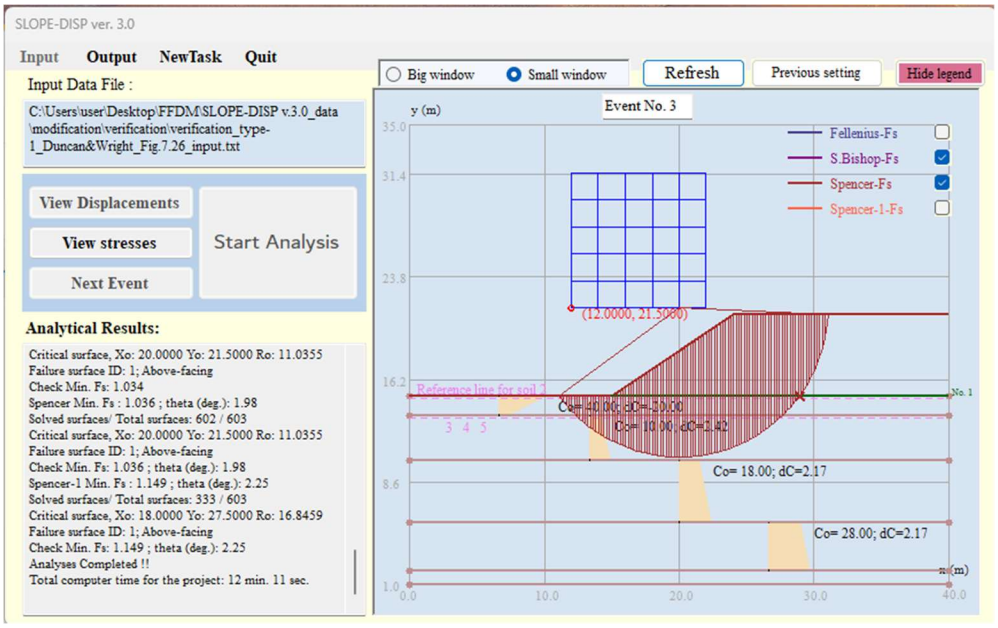

Figure 3.8.4 Critical circular surfaces obtained using Bishop's and Spencer's methods for the case of $T_{allowable}$= 100 kN/m

REFERENCE

Duncan, J.M., Low, B.K., Schaefer, V.R., and Bentler, D.J. (1998). STABGM 2.0- A computer Program for Slope Stability Analysis of Reinforced and Unreinforced Embankments and Slopes. Department of Civil Engineering, Virginia Polytechnic Institute and State University, Blacksburg, VA.

3.9 VERIFICATION CASE STUDY NO. 9

Input and output path: *\SLOPE-ffdm 2.0\Docs\example_verification\Ch3.9

Input: verification_type-1_Duncan&Wright_Fig.7.28_input.txt
Output: verification_type-1_Duncan&Wright_Fig.7.28_output.txt

This case is a hypothetical 24 ft-high reinforced slope backfilled with a cohesionless soil with c= 0 and φ= 37°. A total of five layers of reinforcement with an allowable tensile strength ($T_{allowable}$) of 800 lb/ft. The soil-reinforcement interface adherence is assumed zero, and an interface friction angle of 0.8φ (= 30°). Based on a search from a total of 1994 trial-and-error circles, the minimum values of F_s are shown in Table 3.9.1 and the geometry of critical circle is shown in Fig. 3.9.1. The values of F_s and the geometry of critical arcs obtained in SLOPE-ffdm 2.0 are comparable with those reported in the literature. It is interesting to note that a large reduction of the interface friction angle to 0.3φ (implemented in Event 2 of the analysis) does not change the values of F_s, suggesting that the stability of this slope is not prone to the change of reinforcement-soil interface friction angles. The symbol " x " appeared in Fig. 3.9.1 represents a 'tiebreak' failure mode of reinforcement.

Table 3.9.1 Comparisons of minimum values of F_s obtained in various studies.

	Duncan and Wright (2005)	SLOPE-ffdm 2.0
F_s (Spencer's method)	1.61- 1.71	1.625
F_s (Bishop's method)	---	1.632

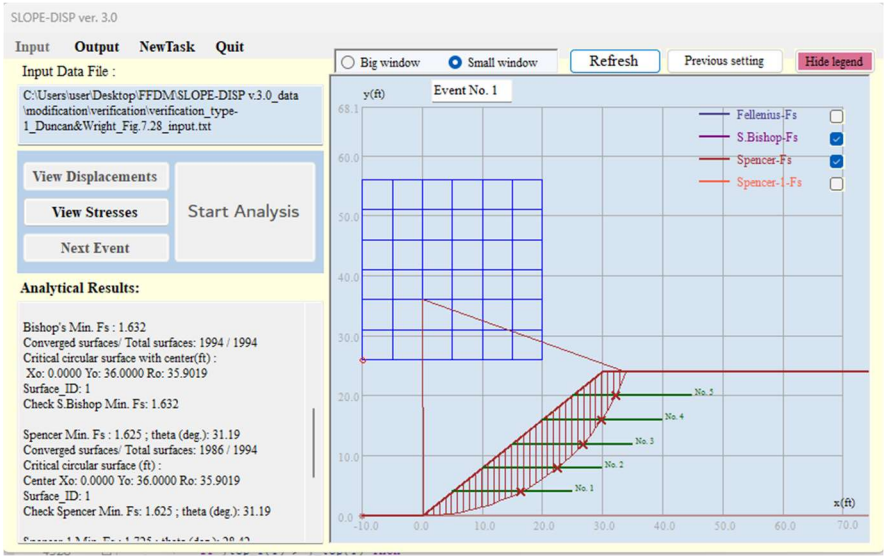

Figure 3.9.1 Critical circular surface for the studied reinforced slope

3.10 VERIFICATION CASE STUDY NO. 10

Input and output path: *\SLOPE-ffdm 2.0\Docs\example_verification\Ch3.10

Input: verification_type-7_Leshchinsky&Huang1992_Fig.6_input.txt
Output: verification_type-7_Leshchinsky&Huang1992_Fig.6_output.txt

This is a case study reported by Chen and Shao (1988) and was re-visited by Leshchinsky and Huang (1992). A deep-seated failure along a weak seam with c= 9.8 kPa, φ=16°. In the above-mentioned studies, straight lines (or wedge-like failures) were used as slip surfaces to describe the failure zone. A slightly different approach is used in the SLOPE-ffdm analysis, i.e., using circular slip lines to replace the straight lines over the weak seam. This type of failure is called 'compound failure' hereafter. The use of arc-like slip lines instead of straight lines is based on the observation that a deep-seated failure in cohesive soils is usually curved, rather than straight ones. Analytical results summarized in Table 3.10.1 supports the use of compound failure surfaces to describe the failure of this slope, i.e., F_s= 0.942 by the rigorous Janbu's method which is marginally smaller than that (F_s= 1.010) reported by Chen and Shao (1988), and F_s= 1.048 by using Spencer's method which is comparable to F_s= 1.061- 1.066 obtained by variational calculus method.

Table 3.10.1 Comparions of F_s obtained using various methods.

	Chen and Shao (1988)	Leshchinsky and Huang (1992)	SLOPE-ffdm 2.0 (Event 1)
Morgenstern-Price	1.010	--	--
Variational Calculus	--	1.061- 1.066	--
Rigorous Janbu	--	1.029	0.942
Spencer	--	--	1.048

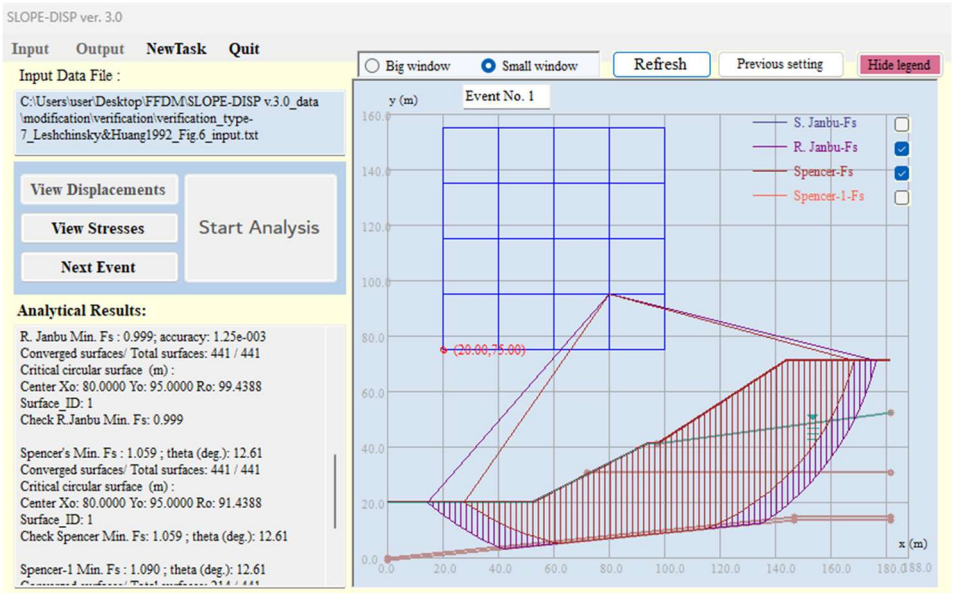

Figure 3.10.1 Critical compound surfaces obtained in SLOPE-ffdm 2.0 analysis

Note that the weak seam in Fig. 3.10.1 is a concave down polyline with gentle slopes. A hypothetical case of a concave up weak seam with a steeper slope is analyzed in Event 2 of analysis to verify the compound surface generation procedure and the analytical results. The resulting values of F_s in comparison with those reported earlier are summarized in Table 3.10.2. The significant influence of the configuration of weak seam can be detected in Table 3.10.2. The critical surfaces shown in Fig. 3.10.2 also reveal the effectiveness of SLOPE-ffdm 2.0 in processing weak seams with complex configurations.

Table 3.10.2 Results of parametric study on the configurations of weak seam using Type-7 analysis of SLOPE-ffdm 2.0.

	Weak seam with gentle slope and concave down weak layer (Event 1; Fig. 3.10.1)	Weak seam with gentle slope and concave upward weak layer (Event 2; Fig. 3.10.2)
Rigorous Janbu	0.942	0.749
Spencer	1.048	0.890

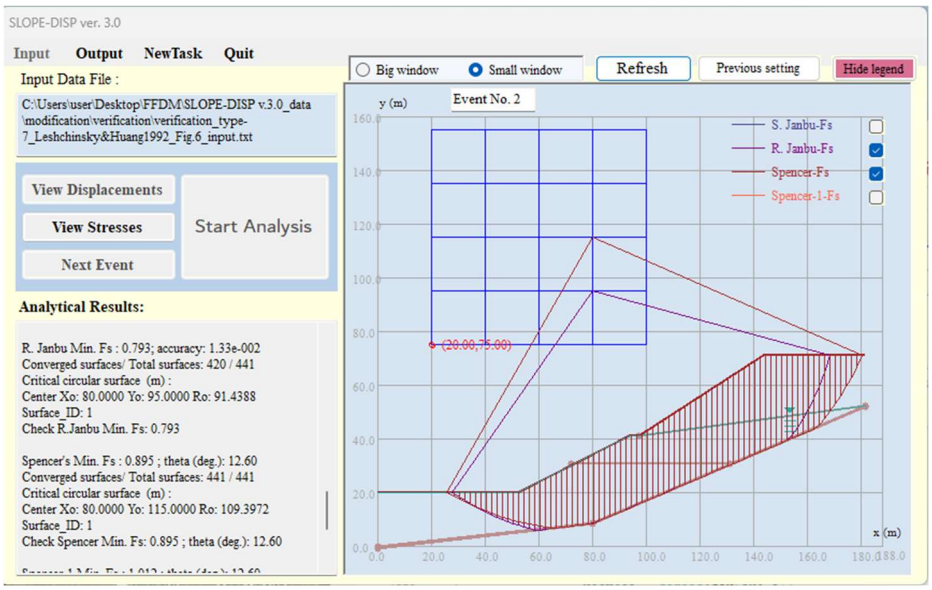

Figure 3.10.2 Critical compound surface in Event 2 analysis for the slope with a concave-upward weak seam.

REFERENCE

Chen, Z.-Y. and Shao, C.-M. (1988) "Evaluatin of minimum factor of safety in slope stability analysis." Candian Geotechnical Journal, Vol. 25, No. 4, pp. 735-748.

Leshchinsky, D. and Huang, C.-C. (1992) "Generalized slope stability analysis: Interpretation, Modification, and Comparison" Journal of Geotechnical Engineering, Vol. 118, No. 10, pp. 1559- 1576.

3.11 VERIFICATION CASE STUDY NO. 11

Input and output path: *\SLOPE-ffdm 2.0\Docs\example_verification\Ch3.11

Input: verification_type-6B_Leshchinsky&Huang1992_Fig.7_input.txt
Output: verification_type-6B_Leshchinsky&Huang1992_Fig.7_output.txt

Input and output path: *\SLOPE-ffdm 2.0\Docs\example_verification\Ch3.11

Input: verification_type-5_Leshchinsky&Huang1992_Fig.7_input.txt
Output: verification_type-5_Leshchinsky&Huang1992_Fig.7_output.txt

This is a case study reported by Chen and Shao (1988) and was later revisited by Leshchinsky and Huang (1992). The multi-layer natural slope subjected to a landslide failure, having an apparent failure surface as shown in Fig. 3.11.1. A Type-6B analysis (for a specific non-circular failure surface described using a polyline) is performed using SLOPE-ffdm 2.0. Calculated values of F_s are compared with those reported in the literature in Table 3.11.1. Results of Type-6B analysis indicate that the value of F_s= 0.794 obtained using the rigorous Janbu's method is deviated from that reported (F_s= 0.863) by Leshchinsky and Huang (1992) by 8%. In general, the values of F_s obtained here are 8-13% smaller than those reported by Leshchinsky and Huang (1992) by using various methodologies.

Table 3.11.1 Comparisons of F_s for the apparent slip surface reported by Chen and Shao (1988)

	Chen and Shao (1988)	Leshchinsky and Huang (1992)	SLOPE-ffdm 2.0 (Type-6B analysis)
Morgenstern-Price	0.917	--	--
Variational Calculus	--	0.876 - 0.889	--
Rigorous Janbu	--	0.863	0.869
Spencer	--	--	0.812

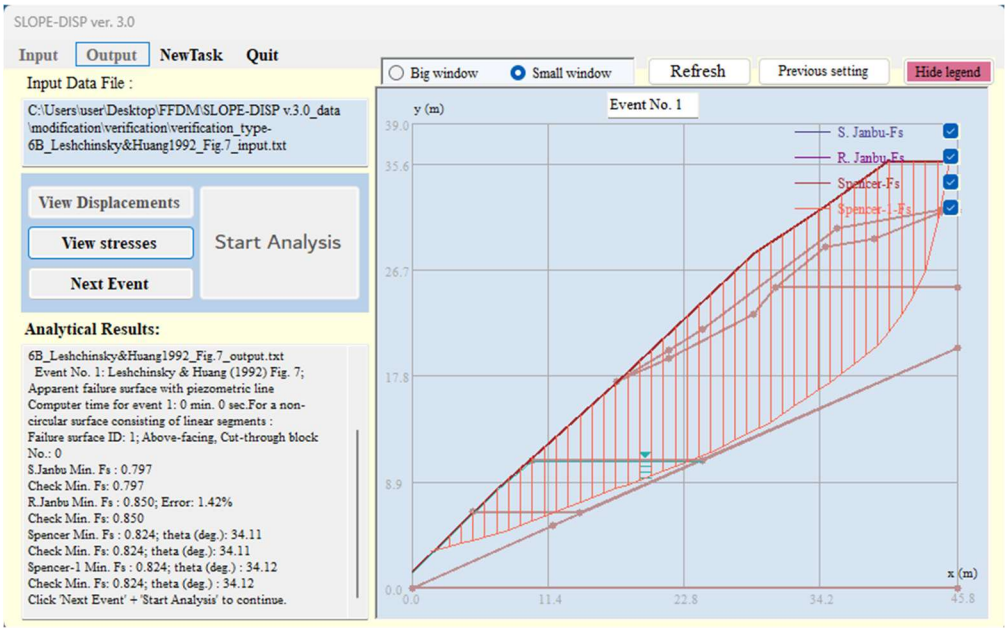

Figure 3.11.1 Results of Type-6B analysis for the apparent failure surface reported by Chen and Shao (1988).

A trial-and-error search for the critical surface and a minimum value of F_s is performed as the event 1 of Type-5 analysis (trial-and-error search using logarithmic spiral surfaces without tension crack). The critical surface found in the analysis is shown in Figs. 3.11.2. A unique critical surface is found, regardless of the methods used. The associated minimum values of F_s are shown in Table 3.11.2. The minimum values of F_s found in the trial-and-error search are 4- 7 % smaller than those obtained in the Type-6B analysis (Table 3.11.1) for the apparent failure surface reported by Chen and Shao (1988). Although the failure mechanism used in Type-5 analysis may be different from that reported by Chen and Shao (1988) which has a close-to-vertical slip surface at the crest, the trial-and-error search using logarithmic failure mechanism is considered as an effective tool in addition to the circular failure used in Type-1, 2 and 3 analyses.

To investigate the influence of tension cracks on the results of slope stability, Event 2 of Type-5 analysis is performed. Introducing a 2.5 m-deep tension crack resulted in 2% lower F_s compared with those without tension crack. Although, this variation of F_s seems small, introducing a tension crack at the crest of slope may improve the situation of unacceptable effective normal stresses at slice base near the crest of the slope, as demonstrated in Figs. 3.11.3 and 3.11.5.

Table 3.11.2 Influence of tension cracks on F_s obtained in trial-and-error logarithmic surface search (Type-5 analysis)

	Type-5 analysis (no tension crack)	Type-5 analysis (with tension crack)
Rigorous Janbu	0.786	0.761
Spencer	0.776	0.755

Figure 3.11.2 Critical surface found in Event 1 of Type-5 analysis (trial-and-error search using logarithmic spiral surfaces without tension crack)

Figure 3.11.3 Critical surface found in Event 2 of Type-5 analysis (trial-and-error search using logarithmic spiral surfaces with a 2.5 m-deep tension crack)

Figures 3.11.4 and 3.11.5 show the normal effective stress at slice base and the inter-slice thrust obtained in R. Janbu's analysis. Negative values of normal stress at

slice base (slice No. 1, 2 from the crest) can be seen. These unacceptable conditions can be alleviated by introducing a 2.5 m-deep tension crack ($2c/\gamma/K_a^{1/2}$ = 3.2 m; c= 19.6 kPa, φ= 21.8 °, γ= 18.1 kN/m^3 , K_a= 0.458) near the crest of the slip surface, as shown in Fig. 3.11.6.

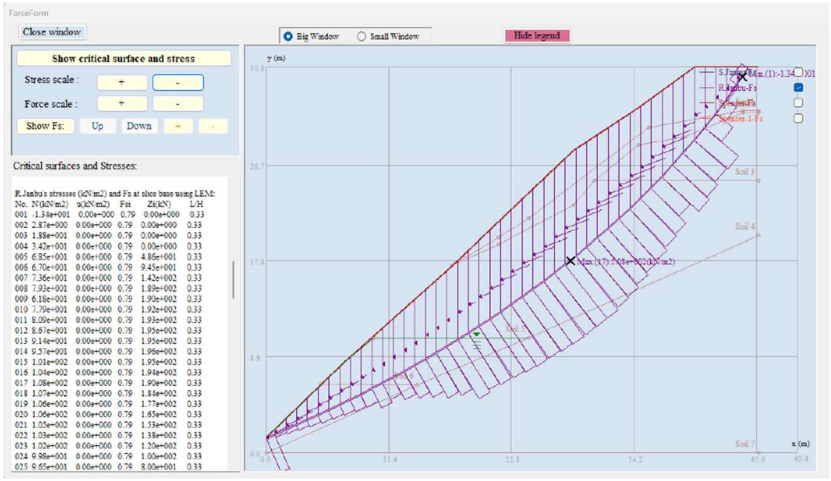

Figure 3.11.4 Effective normal stress at slice base and inter-slice thrust for the critical surface obtained in Rigorous Janbu's method (Event 1, no tension crack)

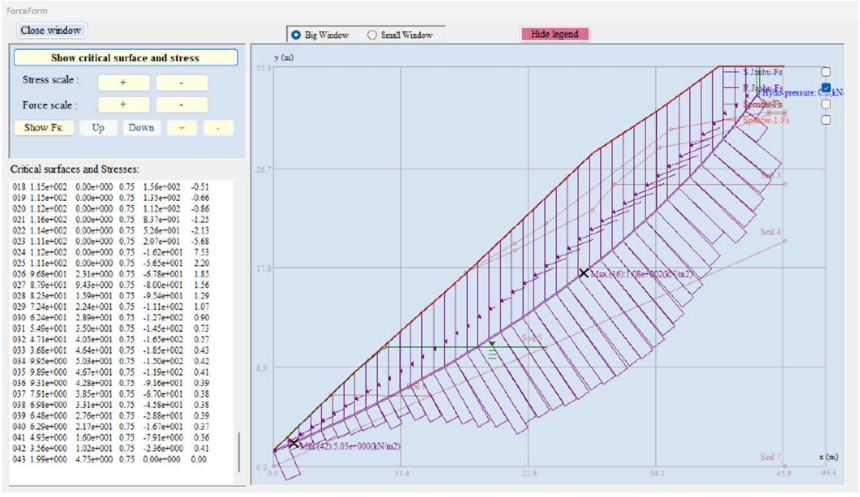

Figure 3.11.5 Effective normal stress at slice base and inter-slice thrust for the critical surface obtained in rigorous Janbu's method (Event 2, with a tension crack)

REFERENCE

Chen, Z.-Y. and Shao, C.-M. (1988) "Evaluation of minimum factor of safety in slope stability analysis." Canadian Geotechnical Journal, Vol. 25, No. 4, pp. 735-748.

Leshchinsky, D. and Huang, C.-C. (1992) "Generalized slope stability analysis: Interpretation, Modification, and Comparison" Journal of Geotechnical Engineering, Vol. 118, No. 10, pp. 1559- 1576.

3.12 VERIFICATION CASE STUDY NO. 12

Input and output path: *\SLOPE-ffdm 2.0\Docs\example_verification\Ch3.12

Input: verification_type-8_Leshchinsky&Huang1992_Fig.8_input.txt
Output: verification_type-8_Leshchinsky&Huang1992_Fig.8_output.txt

This is a 12 m-high, 2:1 (H: V) slope with a known circular (or compound) slip surface with a rotation center at (x= 12.7 m, y= 27.4 m) and a radius of R= 24.4 m. Stability analyses were performed for the slip surface under six groundwater and geological conditions:

Case 1: Homogeneous slope with γ= 18.84 kN/m^3, φ'= 20°, c= 28.7 kPa.

Case 2: Same as Case 1, except with a weak seam (c'=0, φ= 10°).

Case 3: Same as Case 1, except with r_u= 0.25 (r_u: pore pressure ratio, see details in Section 2.5).

Case 4: Same as Case 2, except with with r_u= 0.25.

Case 5: Same as Case 1, except with a piezometric line.

Case 6: Same as Case 2, except with a piezometric line.

In the study using SLOPE-ffdm 2.0, the above Case 1- 6 are analyzed using Event 1 – 6 in the input data file. The results are summarized in Table 3.12.1. Comparisons of Fs obtained by the Morgenstern-Price and those by the Spencer method reveal that the differences are less than 1.8%. Comparisons of Fs obtained using R. Janbu's in SLOPE-ffdm 2.0 are comparable to those reported by Leshchinsky and Huang (1992) using R. Janbu's and variational calculus methods with differences between -4% ~ +6%, only with one exception of Case 6 for which F_s= 1.182 obtained here is about 9% smaller than F_s= 1.298 reported by Leshchinsky and Huang (1992).

Figures 3.12.1 and 3.12.2 shows results of Case 5 and Case 6, respectively, analyses. Fig. 3.12.1 highlights a special technique regarding the input data, i.e., to implement the Type-8 (or Type-7) analysis, it is necessary to incorporate a weak seam (or weak layer) in the slope profile. This seems contradictory to the geological condition of Case 5 in which a weak seam is non-existent. To clear this issue, a weak seam is intentionally located at a deep location out of the reach of all trial-and-error surfaces. Results of using this technique can be seen in Fig. 3.12.1 in which a weak layer of about 1 m-thick (the thickness can be arbitrarily chosen; in Fig. 3.12.2, a 0.1 m-thick weak seam is used) is incorporated.

Table 3.12.1 Comparisons of F_s obtained for Case 1- 6 reported by Fig. 8 of Leshchinsky and Huang (1992)

	Fredlund and Krahn (1977)	Leshchinsky and Huang (1992)		SLOPE-ffdm 2.0 (Type-8 analysis)	
	Morgenstern-Price Inter-slice function $f(x)$= 1	R. Janbu	Variational Calculus	R. Janbu	Spencer
Case 1	2.076	2.008	2.053-2.080	2.098	2.104
Case 2	1.378	1.432	1.312-1.333	1.368	1.359
Case 3	1.765	1.708	1.739-1.765	1.781	1.784
Case 4	1.124	1.162	1.067-1.080	1.144	1.141
Case 5	1.833	1.776	1.813-1.839	1.849	1.843
Case 6	1.250	1.298	1.181-1.197	1.278	1.264

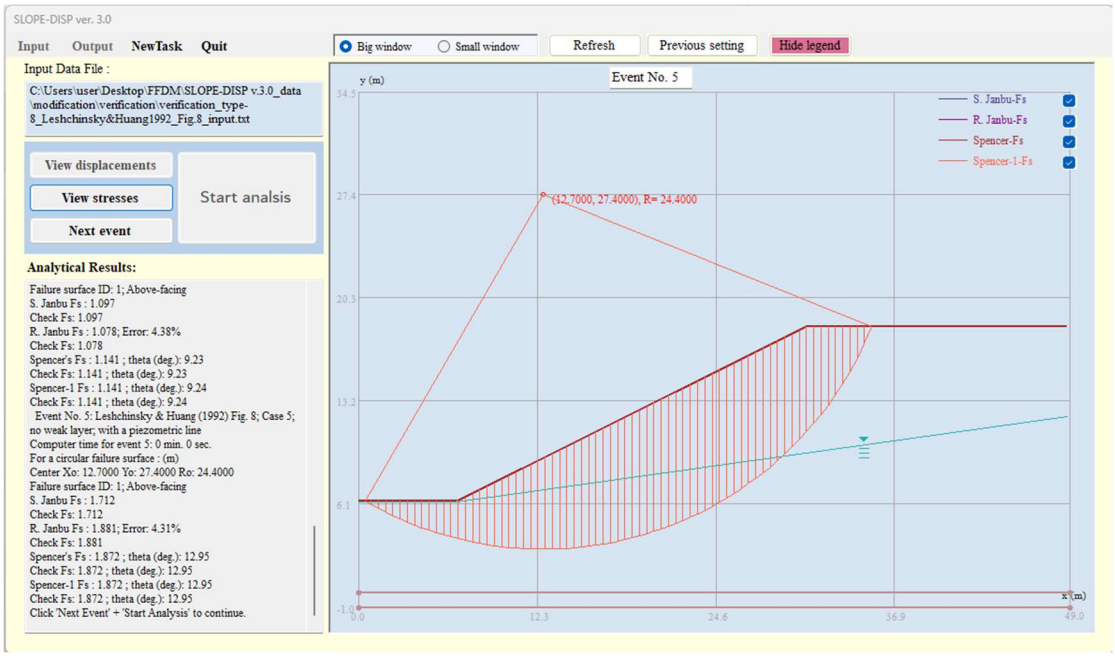

Figure 3.12.1 Results of Type-8 analysis for Case 5 of Fig. 8 reported by Leshchinsky and Huang (1992)

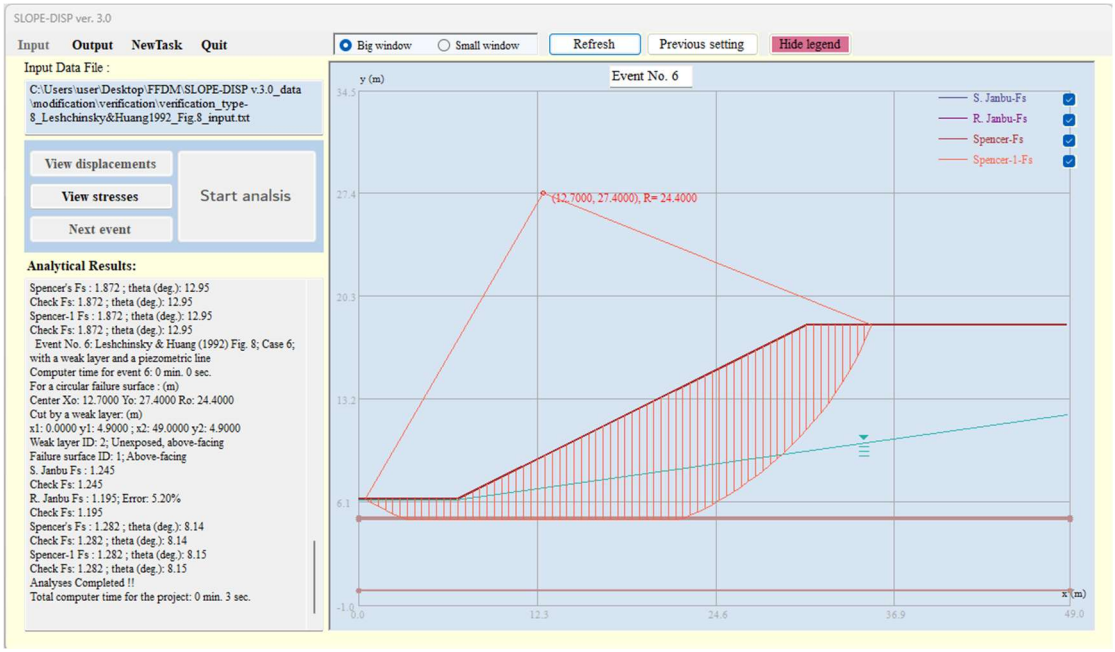

Figure 3.12.2 Results of Type-8 analysis for case 6 of Fig. 8 reported by Leshchinsky and Huang (1992)

The following generalized interslice function has been proposed by Spencer (1973) and Mogenstern and Price (1980??). In which, f(xi) can be an arbitrary function:

$$\tan \delta_i = f(x_i) \tan \theta \qquad (3-12-1)$$

One of the following three types of $f(x)$ can be assigned by the users of SLOPE-ffdm 2.0:

Type-1: $f(x_i)$= 1; this is the default of the computer program, generating a constant inclination angle $\delta_i = \theta$ (i= 1--- ns) throughout the sliding mass , $0 \leqq x_i \leqq 1$ (x_i: normalized x-coord. of slice No. i).

Type-2: $f(x_i) = sin(\pi x_i)$; this is a half-sine function; $0 \leqq f(x_i) \leqq 1$, $0 \leqq x_i \leqq 1$.

Type-3: $f(x_i)$ is defined by a polyline with a total number of points, n, and their coordinates (x_i, y_i); $0 \leqq x_i \leqq 1$ and $0 \leqq y_i \leqq 1$; x_i: the normalized x-coord.; y_i: inter-slice force function.

In general, the use of $f(x_i)$=1.0 generates good results of F_s. Mogenstern and Price (1965) proposed the use of a half-Sine inter-slice function to obtain an acceptable result of slope stability analysis. Spencer (1973) has demonstrated the effectiveness of using various functions of $f(x_i)$ to improve the rationality of inter-slice thrust height

distributions. In the following analyses, the Type-2 inter-slice function defined as following is used:

$$f(x_i) = \sin\left[\pi \cdot \frac{(W - D_i)}{W}\right] \qquad (3-12-2)$$

W: the full width of the slip surface

D_i: distance between slice No. i and the toe of the slip surface

Table 3.12.2 shows a comparison of the values of F_s between those reported by Fredlund and Krahn (1977) and SLOPE-ffdm 2.0 for Case 1- 6. The values of F_s obtained here are within a negligibly small range of ±2% compared to those reported by Fredlund and Krahn (1977).

Table 3.12.2 Comparisons of F_s obtained in different studies with a half-Sine interslice function

	Fredlund and Krahn (1977)	SLOPE-ffdm 2.0 (Type-8 analysis)
Methods	Morgenstern-Price method	Spencer's method
Case 1	2.076	2.104
Case 2	1.378	1.350
Case 3	1.764	1.784
Case 4	1.118	1.129
Case 5	1.832	1.843
Case 6	1.245	1.255

REFERENCE

Chen, Z.-Y. and Shao, C.-M. (1988) "Evaluatin of minimum factor of safety in slope stability analysis." Candian Geotechnical Journal, Vol. 25, No. 4, pp. 735-748.

Fredlund, D.G. and Krahn, J. (1977) "Compariso of slope stability methods of analysis" Candian Geotechnical Journal, Vol. 14, No. 3, pp. 429-439.

Leshchinsky, D. and Huang, C.-C. (1992) "Generalized slope stability analysis: Interpretation, Modification, and Comparison" Journal of Geotechnical Engineering, Vol. 118, No. 10, pp. 1559- 1576.

Mogenstern, N.R. and Price, V.E. (1965) "The analysis of stability of general slip surfaces" Geotechnique, Vol. 15, No.1, pp. 79-93.

3.13 VERIFICATION CASE STUDY NO. 13

Input and output path: *\SLOPE-ffdm 2.0\Docs\example_verification\Ch3.13

Input: verification_type-8_spencer1973_ns=102_input.txt Output: verification_type-8_spencer1973_ns=102_output.txt
Input: verification_type-8_spencer1973_ns=16_input.txt Output: verification_type-8_spencer1973_ns=16_output.txt

This case study, originally presented by Spencer (1973), examines a homogeneous gentle slope composed of *c-φ* soil. The study explores the effects of varying the inter-slice force function, *k(x)*, and the depth of the tension crack, z_t, on several critical parameters: the safety factor (F_s), the value of $tan\theta$, the inter-slice force (Z_i), and the height of the normal component of the inter-slice force from the base of each slice (L_i).

Table 3.13.1 presents a comparison of F_s and $tan\theta$ values as reported by Spencer (1973) and those generated using SLOPE-ffdm 2.0. As shown in Table 3.13.1, SLOPE-ffdm 2.0 yields more responsive results for F_s and $tan\ \theta$, particularly when tension crack depths and inter-slice force functions *k(x)* are varied. These discrepancies are attributed to advancements in computational techniques across different eras.

Overall, the accuracy of both the analytical formulations discussed herein and the performance of the SLOPE-ffdm 2.0 program has been verified, confirming its effectiveness in producing reliable and adaptable outputs in slope stability analyses.

Table 3.13.1 Comparisons of F_s and tan θ obtained in various studies

Input conditions			Spencer (1973) *ns* = 16		SLOPE-ffdm 2.0 *ns* = 16		SLOPE-ffdm 2.0 *ns* = 102	
Event	z_t/H	*k(x)* type	F_s	$tan\ \theta$	F_s	$tan\ \theta$	F_s	$tan\ \theta$
1	0	1	1.46	0.26	1.462	0.253	1.462	0.255
2	0.1	1	1.46	0.26	1.450	0.252	1.453	0.258
3	0.2	1	1.46	0.26	1.446	0.249	1.450	0.259
4	0.3	1	1.46	0.26	1.448	0.246	1.455	0.259
5	0.2	2	1.46	0.27	1.444	0.255	1.451	0.270
6	0.2	3	1.46	0.36	1.447	0.346	1.454	0.368

Figure 3.13.1 illustrates the slope and slice configuration (n_s = 16) used in the analysis of Event 3, consistent with the parameters reported by Spencer (1973). The corresponding stress distribution is presented in Figure 3.13.2. Notably, several lateral thrust application points near the crest appear to fall below the slip surface.

By contrast, when the number of slices is increased to n_s = 102—as shown in Figures 3.13.3 and 3.13.4—the thrust application points shift upward, aligning more closely with approximately one-third of each slice's side face. This refinement in thrust localization results from improved accuracy in the moment equilibrium equations, wherein the slice base is modeled as a straight line rather than an arc.

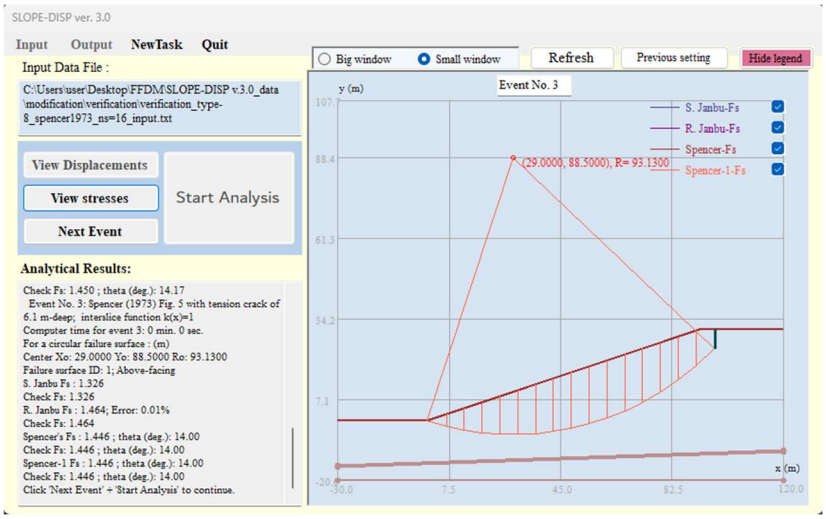

Figure 3.13.1 Results of Event 3 analysis using *ns*= 16 in SLOPE-ffdm 2.0 for the slope reported by Spencer (1973).

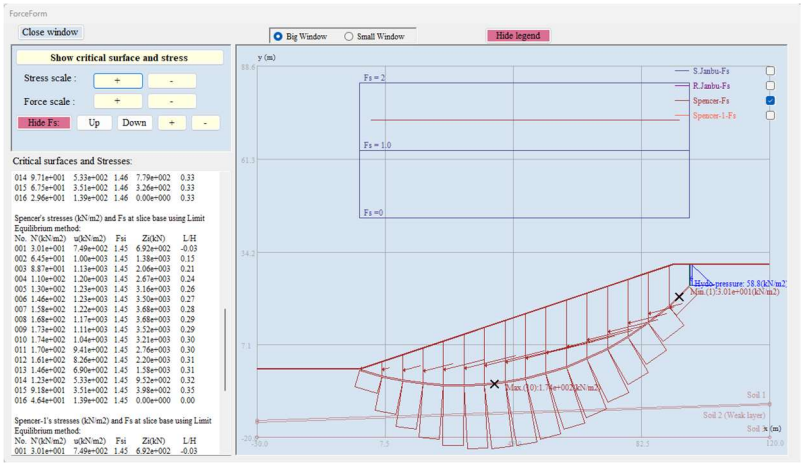

Figure 3.13.2 Results of stress analysis for Event 3 analysis using *ns*= 16 in SLOPE-ffdm 2.0 for the slope reported by Spencer (1973).

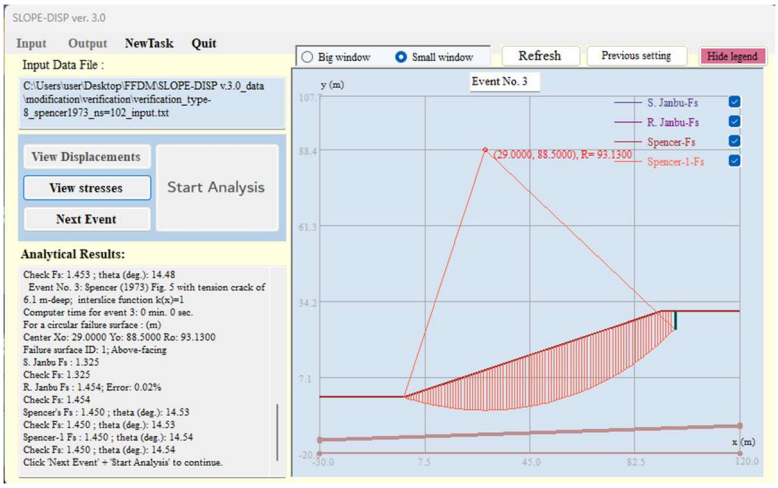

Figure 3.13.3 Results of Event 3 analysis using *ns*= 102 in SLOPE-ffdm 2.0 for the slope reported by Spencer (1973).

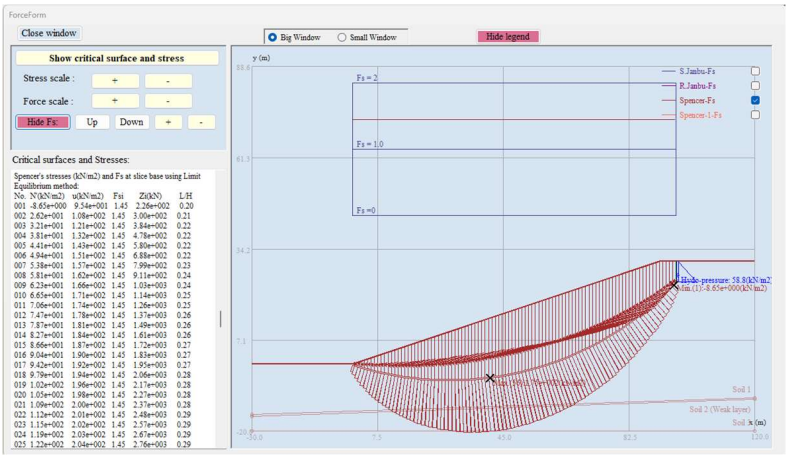

Figure 3.13.4 Results of stress analysis for Event 3 analysis using *ns*= 102 in SLOPE-ffdm 2.0 for the slope reported by Spencer (1973).

In addition to the safety factor (F_s) and the value of $tan\theta$, the output data file includes several other parameters: effective normal stress (N_i'), porewater pressure acting on the slice base (U_i), inter-slice total force (Z_i), and the inter-slice thrust height ratio (h_i/H_i). By default, SLOPE-ffdm 2.0 applies not only Spencer's method, but also the simplified and rigorous versions of Janbu's method concurrently to the same potential failure surface. This multi-method approach allows comparative analysis, supporting a more informed and balanced final engineering judgment.

REFERENCES

Spencer, E. (1973). Thrust line criterion in embankment stability analysis. Geotechnique, 23, No. 1, 85-100.